JOC*Article*

A Theoretical Study of the Mechanism of Selective Fluorination of Saturated Hydrocarbons by Molecular Fluorine. Participation of $CHCl_3$ Solvent Molecules in the Ionic Process

Haruhiko Fukaya[†,‡] and Keiji Morokuma*[,‡]

Institute for Structural and Engineering Materials, National Institute of Advanced Industrial Science and Technology (AIST), Shimoshidami, Moriyama-ku, Nagoya 463-8560, Japan, and Department of Chemistry and Cherry L. Emerson Center for Scientific Computation, Emory University, 1515 Pierce Drive., Atlanta, Georgia 30322

morokuma@emory.edu

Received May 30, 2003

The fluorination reaction of methane and isobutane by molecular F_2 with and without $CHCl_3$ solvent was studied with the ab initio and ONIOM theoretical calculations. The electrophilic pathway for the RH + F_2 reaction in general is a two-step process, consisting of hydride abstraction leading to an intermediate of the type $R^{+\delta}\cdots HF\cdots F^{-\delta}$, followed by complicated rearrangement to give the electrophilic substitution product, RF + HF. In the case of methane, the overall barrier for this reaction is too high for the reaction to take place under mild conditions even in the presence of $CHCl_3$ solvent molecules. In the case of isobutane without $CHCl_3$, the electrophilic pathway has a high rate-determining barrier of 25 kcal/mol, and is not likely to take place; the radical process forming *t*-Bu$^\bullet$ + HF + F$^\bullet$ may be preferred. However, the *t*-$Bu^{+\delta}\cdots HF\cdots F^{-\delta}$ intermediate and, in particular, the transition state **TS2** for rearrangement of the intermediate are highly ionic, and are stabilized dramatically when a few $CHCl_3$ solvent molecules form a solvation cage. The electrophilic reaction for isobutane + F_2 has a low overall barrier when at least three $CHCl_3$ molecules are present and can take place under mild conditions with full retention of configuration.

Introduction

Molecular fluorine is very reactive because the F−F bond energy is remarkably low (37.9 kcal/mol)[1] and the fluorine atom forms a strong bond with other elements, e.g., the C−F bond energy is about 120 kcal/mol.[2] For instance, the reaction of organic compounds with neat F_2 proceeds vigorously in an uncontrollable manner, and a variety of products are formed via radical chain reactions. At the beginning of the 1970s, however, Adcock and Lagow showed that the direct fluorination of organic compounds by a fluorine molecule successfully occurred under low F_2 concentrations and low temperatures.[3] In this reaction, fluorine could replace all the hydrogens in a given organic molecule, thus affording perfluoro derivatives, which are useful for the development of fluorinated solvents, polymers, and other reagents.

On the other hand, since monofluorinated compounds have biological activity,[4] selective fluorination is also important for development of new drugs. Rozen et al. showed that the selective substitution of the tertiary C−H bond proceeded with full retention of configuration by elemental fluorine in a polar solvent, while the same kind of reaction produced fluorine-containing tars when it occurred in a nonpolar solvent (−70 °C, 2−4% F_2 in N_2).[5] The polar solvent, $CHCl_3$, plays the important role: it is a good radical scavenger, it provides a polar medium, and it acts as an acceptor for the developing F anion through hydrogen bonding. They proposed a mechanism via a pentacoordinated carbonium ion transition state, as shown in Scheme 1.[6]

SCHEME 1

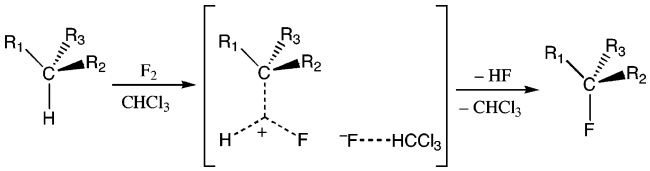

Although there are many theoretical studies of the reaction of fluorine atom and fluoride ion with methane,[7] only one report by Kaneko et al. has appeared on the theoretical approach to the electrophilic fluorination of

† AIST.
‡ Emory University.

(1) *CRC Handbook of Chemistry and Physics*, 82nd ed.; Lide, D. R., Ed.; CRC Press: Boca Raton, FL, 2001; Chapter 5.
(2) (a) Banks, R. E. In *Fluorine the First Hundreds Years*; Banks, R. E., Sharp, D. W. A., Tatlow, J. C., Eds.; Elsevier Sequoia: Lausanne and New York, 1986; Chapter 1. (b) Banks, R. E.; Tatlow, J. C. In *Fluorine the First Hundreds Years*; Banks, R. E., Sharp, D. W. A., Tatlow, J. C., Eds.; Elsevier Sequoia: Lausanne and New York, 1986; Chapters 4 and 11.
(3) Adcock, J. L.; Lagow, R. J. *J. Am. Chem. Soc.* **1974**, *96*, 7589.
(4) Filler, R. In *Fluorine the First Hundreds Years*; Banks, R. E., Sharp, D. W. A., Tatlow, J. C., Eds.; Elsevier Sequoia: Lausanne and New York, 1986; Chapter 13.
(5) Rozen, S. *Acc. Chem. Res.* **1988**, *21*, 307.
(6) (a) Rozen, S.; Ben-Shushan, G. *J. Org. Chem.* **1986**, *51*, 3522. (b) Rozen, S.; Gal, C. *J. Org. Chem.* **1987**, *52*, 2769. (c) Gal, C.; Rozen, S. *Tetrahedron Lett.* **1985**, *26*, 2793.

10.1021/jo034740c CCC: $25.00
Published on Web 09/24/2003

methane with molecular fluorine.[8] They analyzed the entire process of the direct fluorination of methane at the HF/6-311++G** level. However, the reaction they calculated did not take place in the experiment, and their approach was unable to answer the mechanistic question of whether the direct fluorination is electrophilic or radical substitution.[9] In the present study, we will examine the system of CH_4 (sometimes abbreviated as MeH) or $(CH_3)_3CH$ (abbreviated as *t*-BuH) + F_2 + $n$$CHCl_3$ (n = 0 to 3), including up to three solvent $CHCl_3$ molecules explicitly in the calculation, and clarify the mechanism of the direct fluorination in solution.

Computational Methods

Ab initio electronic structure calculations were performed with the Gaussian 98 program package.[10] All geometries were optimized by the second-order Møller−Plesset (MP2) method[11] with the mixed basis set 6-31+G* for the fluorine atom and 6-31G* for the others; we will call this basis set 6-31+(F)G*. The diffuse function on F is intended to describe any anionic character that any F atom may take during the reaction process. At the optimized stationary points, the analytical MP2 second derivatives were used to calculate vibrational frequencies and zero-point energies (ZPE) at the level used for optimization. The atomic charges were calculated by the natural bond orbital (NBO) analyses.[12]

The effects of the basis set on the geometries and relative energies were tested for a transition state **TS2** as well as the reactants, as shown in Figure S1 in the Supporting Information. The diffuse function is important in this system: MP2/6-31G* lacking diffuse functions gave the energy of **TS2** (relative to the reactants) higher by as much as 15 kcal/mol compared with MP2/6-31+G*. As seen in the NBO population in Figure S1, **TS2** has a substantial ionic character, especially for F atoms, and anions cannot be described properly without diffuse functions. To test whether diffuse functions are needed for all the atoms, we adopted the mixed basis set MP2/6-31+(F)G* in which the diffuse function was assigned to only fluorine atoms. The optimized geometry and the relative energy with MP2/6-31+(F)G* are very similar to those with MP2/6-31+G*, and therefore we decided to use the MP2/6-31+(F)G* method for the geometry optimizations. Table S1 in the Supporting Information shows the energies of transition states calculated by the MP2/6-31+G* and MP2/6-31+(F)G* methods accompanied by the single-point calculation at the MP2/6-31+G* on the geometry optimized by MP2/6-31+(F)G*. Because the MP2/6-31+G*//MP2/6-31+(F)G* gave results closer to the MP2/6-31+G*//MP2/6-31+G* than the MP2/6-31+(F)G*//MP2/6-31+(F)G* results, we decided to choose the MP2/6-31+G*//MP2/6-31+(F)G* method.

The calculations including one to three molecules of $CHCl_3$ were performed with the ONIOM method,[13] as pure MP2 calculations for these systems were too time-consuming for our computational resources. We used the two-layer ONIOM, where $CHCl_3$ molecules were replaced by HF or HCl in the "model" system treated at the "high" level. Table S2 in the Supporting Information shows the results of the activation energy for the second step of the reaction of *t*-BuH + F_2 + $CHCl_3$. The ONIOM calculation with HCl as the "model" of $CHCl_3$ without diffuse function, ONIOM(MP2/6-31G*:HF/6-31G*), gave higher relative energies of about 13 kcal/mol in **INT** and 22 kcal/mol in **TS2** compared with the MP2/6-31+G*//MP2/6-31+(F)G* method, resulting in the **INT** → **TS2** activation energy being higher by about 10 kcal/mol. The ONIOM calculation including diffuse function, ONIOM(MP2/6-31+G*:HF/6-31+G*), also gave a few kilocalories/mole higher relative energies compared with the MP2/6-31+G//MP2/6-31+(F)G* method; however, the ONIOM **INT**→**TS2** activation energy was within 1 kcal/mol error relative to the MP2. We tested for two "models" of H−CCl_3, i.e., H−F and H−Cl, to be treated at the "high" level in the ONIOM calculation. As seen in Table S2, the H−Cl model was slightly better than the H−F model. The hydrogen Mulliken atomic charges (and dipole moments, in Debye) of $CHCl_3$, HCl, and HF calculated at the HF/6-31+G* level are 0.32 (1.34), 0.23 (1.53), and 0.56 (2.08), respectively. Because the charge on the H atom and dipole moments of HCl were close to those of $CHCl_3$ compared with HF, the electrostatic effect of HCl on the reaction center was closer to $CHCl_3$ than that of HF. This could be a reason why HCl was a better model for $CHCl_3$ than HF. However, since the activation energies calculated by both models differ by only 0.2 kcal/mol, we chose the cheaper HF model.

Results and Discussions

A. Reaction of CH_4 + F_2. At first we will study the reaction of CH_4 with F_2, without the intervention of any $CHCl_3$ solvent molecule, as the simplest system. A weak pre-reaction van der Waals complex **MF_RC** was found between the reactants, as shown in Figure S2 in the Supporting Information. Two transition states, **MF_TS1** and **MF_TS2**, were found with the MP2 calculation, in contrast to the HF level calculation that gave only one transition state.[8] The first MP2 transition state **MF_TS1** has near C_{3v} symmetry, and the C−H and the F−F bonds were elongated by 11% and 19%, respectively, relative to the reactants. The reaction coordinate indicates that this is the transition state for the simultaneous abstraction of H from CH_4 (to form HF) and the dissociation of the F−F bond. The IRC calculation[14] confirmed that this transition state actually connects **MF_RC** and **MF_INT**. Further elongation of the C−H and the F−F bonds was found in the intermediate **MF_INT**, and a small stabilization of 1.7 kcal/mol takes place, as shown in Figure 1. The H−F1 bond is nearly formed, with its bond distance only 11% longer than in isolated HF, and F2 has nearly half of the minus charge (−0.40e). In the second transition state **MF_TS2**, the major component of the reaction coordinate is the rotation of the H−F1

(7) (a) Davis, L. P.; Burggraf, L. W.; Gordon, M. S.; Baldridge, K. K. *J. Am. Chem. Soc.* **1985**, *107*, 4415. (b) Corchado, J. C.; Espinosa-Garcia, J. *J. Chem. Phys.* **1996**, *105*, 3152. (c) Corchado, J. C.; Espinosa-Garcia, J. *J. Chem. Phys.* **1996**, *105*, 3160. (d) Pais, A. A. C. C.; Arnaut, L. G.; Formosinho, S. J. *J. Chem. Soc., Perkin Trans. 2* **1998**, 2577.

(8) Kaneko, C.; Toyota, A.; Chiba, J.; Shigihara, A.; Ichikawa, H. *Chem. Pharm. Bull.* **1994**, *42*, 745.

(9) Chambers, R. D.; Parsons, M.; Sandford, G.; Bowden, R. *Chem. Commun.* **2000**, 959.

(10) Frisch, M. J.; Trucks, G. W.; Schlegel, H. B.; Scuseria, G. E.; Robb, M. A.; Cheeseman, J. R.; Zakrzewski, V. G.; Montgomery, J. A., Jr.; Stratmann, R. E.; Burant, J. C.; Dapprich, S.; Millam, J. M.; Daniels, A. D.; Kudin, K. N.; Strain, M. C.; Farkas, O.; Tomasi, J.; Barone, V.; Cossi, M.; Cammi, R.; Mennucci, B.; Pomelli, C.; Adamo, C.; Clifford, S.; Ochterski, J.; Petersson, G. A.; Ayala, P. Y.; Cui, Q.; Morokuma, K.; Malick, D. K.; Rabuck, A. D.; Raghavachari, K.; Foresman, J. B.; Cioslowski, J.; Ortiz, J. V.; Stefanov, B. B.; Liu, G.; Liashenko, A.; Piskorz, P.; Komaromi, I.; Gomperts, R.; Martin, R. L.; Fox, D. J.; Keith, T.; Al-Laham, M. A.; Peng, C. Y.; Nanayakkara, A.; Gonzalez, C.; Challacombe, M.; Gill, P. M. W.; Johnson, B. G.; Chen, W.; Wong, M. W.; Andres, J. L.; Head-Gordon, M.; Replogle, E. S.; Pople, J. A. *Gaussian 98*, revision A.7; Gaussian, Inc.: Pittsburgh, PA, 1998.

(11) Møller, C.; Plesset, M. S. *Phys. Rev.* **1934**, *46*, 618.

(12) (a) Foster, J. P.; Weinhold, F. *J. Am. Chem. Soc.* **1980**, *102*, 7211. (b) Reed, A. E.; Weinstock, R. B.; Weinhold, F. *J. Chem. Phys.* **1985**, *83*, 735. (c) Reed, A. E.; Curtiss, L. A.; Weinhold, F. *Chem. Rev.* **1988**, *88*, 899.

(13) Maseras, F.; Morokuma, K. *J. Comput. Chem.* **1995**, *16*, 1170.

(14) (a) Fukui, K. *Acc. Chem. Res.* **1981**, *14*, 363. (b) Gonzalez, C.; Schlegel, H. B. *J. Chem. Phys.* **1989**, *90*, 2154. (c) Gonzalez, C.; Schlegel, H. B. *J. Chem. Phys.* **1990**, *94*, 5523.

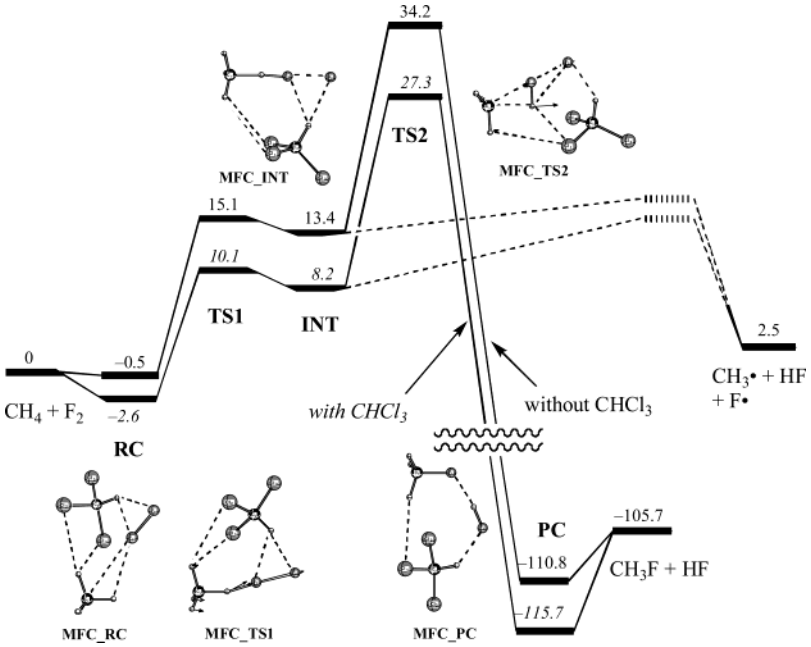

FIGURE 1. Potential energy profiles (in kcal/mol, with ZPE) for the reaction of $CH_4 + F_2$ with (in italic) and without $CHCl_3$ at the MP2/6-31+G*//MP2/6-31+(F)G* level. Sketches of the structures are for $CH_4 + F_2 + CHCl_3$ at the MP2/6-31+(F)G* level taken from Figure S3.

fragment, with the F1 end being attracted toward C (eventually to form a F−C bond) and the positively charged (+0.50e) H end approaching F2, which is strongly anionic with a charge of −0.78e (to break the H−F1 bond and from a new H−F2 bond). The IRC calculation confirms that **MF_TS2** connects **MF_INT** and the product complex **MF_PC**, which is a van der Waals complex between HF and CH_3F. Overall the reaction is the exchange of one H and one F atom between CH_4 and F_2. However, this takes place via an intermediate **MF_INT**, an unusual complex that can be described as $CH_3^{+\delta}\cdots HF\cdots F^{-\delta}$. It should be noted that during the present ionic process, the CH_3 group remains pyramidalized and its absolute configuration is retained. The reaction coordinate at TS is clearly the rotation of the HF molecule, which brings H closer to F2 and later causes the H−F2 as well as the F1−C bond formation.

The activation barrier (including ZPE) for the first step, for formation of a not so stable intermediate **MF_INT** by braking a C−H and a F−F bond and forming a H−F bond, is 15.6 kcal/mol. The barrier for the second step, for braking of the H−F bond and formation of a new H−F bond and a C−F bond, is 20.8 kcal/mol. Since the reverse barrier from the intermediate **MF_INT** is so small (1.7 kcal/mol), the overall activation process should be considered to be a single step from **MF_RC** to **MF_TS2**, with the overall barrier of 34.7 kcal/mol. The reaction therefore is not expected to take place under mild conditions.

In Figure 1, we also included possible radical dissociation products, $^{\bullet}CH_3 + HF + F^{\bullet}$, from the $CH_3\cdots HF\cdots F$ intermediate **INT**. Since the energy of the products is lower than that of **INT**, there must be a transition state between the two. However, we did not locate it, as our primary concern was the path leading directly to CH_3F + HF. We just mention that in the present system without $CHCl_3$ solvent this radical dissociation pathway may compete against the ionic pathway through **TS2**.

B. Reaction of $CH_4 + F_2 + CHCl_3$. The above results suggest the existence of a very polar species such as **MF_INT** during the reaction, and therefore the direct participation of the polar solvent molecules of $CHCl_3$ in the reaction may have to be considered. For this purpose, we have added one $CHCl_3$ molecule in the reaction system of $CH_4 + F_2$. The optimized geometries of stationary points are shown in Figure S3 in the Supporting Information and sketched in Figure 1. The addition of $CHCl_3$ to the reaction system causes rather small changes in optimized geometries. In all the structures the $CHCl_3$ molecule seems to coordinate with the most negatively charged atom of the system with its positively charged H atom. However, in no case does it seem to participate directly in the reaction coordinate. The transition state **MFC_TS1** is a little earlier compared with **MF_TS1**, with shorter C−H and F−F bonds and a longer H−F bond. The intermediate, **MFC_INT**, also seems to be in an earlier stage of reaction than **MF_INT** with shorter C−H and F−F bonds and a longer H−F bond. As shown in Figure 1, energetically, all species are stabilized by "solvation" by $CHCl_3$: 2.0, 5.0, 5.2, 6.9, and 4.9 kcal/mol for **MFC_RC**, **MFC_TS1**, **MFC_INT**, **MFC_TS2**, and **MFC_PC**, respectively. The most polar species **MFC_TS2** is most strongly stabilized. This will reduce the overall barrier for **RC** → **TS2** from 34.7 kcal/mol without $CHCl_3$ to 29.8 kcal/mol with $CHCl_3$. However, the barrier is still high and the reaction remains inaccessible under mild conditions.

C. Reaction of $(CH_3)_3CH + F_2$. The reaction we have so far studied for methane experimentally takes place only for compounds with a tertiary C−H bond. Therefore, we now study the reaction of isobutane ($(CH_3)_3CH$) with F_2. The optimized geometries of the stationary points for the reaction $(CH_3)_3CH + F_2$ are shown in Figure S4 in

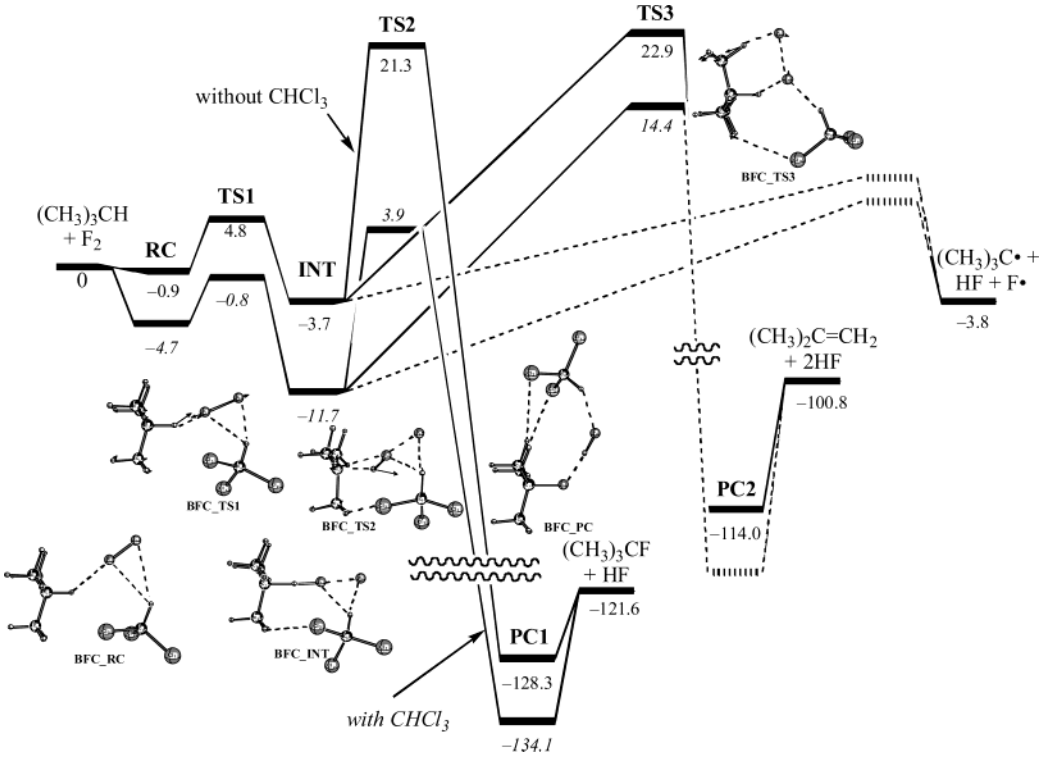

FIGURE 2. Potential energy profiles (in kcal/mol, with ZPE) for the reaction of $(CH_3)_3CH + F_2$ with (in italic) and without $CHCl_3$ at the MP2/6-31+G*//MP2/6-31+(F)G* level. Sketches of the structures are for $(CH_3)_3CH + F_2 + CHCl_3$ at the MP2/6-31+(F)G* level taken from Figure 3.

the Supporting Information. The qualitative features of these structures are very similar to those for $CH_4 + F_2$. The transition state **BF_TS1** has nearly C_{3v} symmetry like **MF_TS1**, but the former is earlier than the latter: the C−H bond of **BF_TS1** was elongated only by 5% and the F−F by 12%, vs 11% and 19%, respectively, in **MF_TS1**. The intermediate **BF_INT** has shorter C−H and F−F bonds and a longer H−F bond compared with **MF_INT**. Although **BF_INT** has a more reactant-like structure than **MF_INT**, F2 has more negative charge, −0.45e, compared with that in **MF_INT**, −0.40e. The electron-donating character of the three CH_3 groups in *tert*-butyl may be responsible for the larger charge transfer to F2. The C−H bond length in **BF_TS2**, 55% elongated compared with the reactant, is shorter than that in **MF_TS2**, 89% elongated. The F−F bond in **BF_TS2** is longer than that in **MF_TS2**, and F2 has a large negative charge, −0.88e. We note that the *tert*-butyl group, always interacting with the other parts of the system, remains pyramidalized and retains its absolute configuration during the reaction. The reaction coordinate at TS is clearly the rotation of the HF molecule, which brings H closer to F2 and later causes the H−F2 as well as F1−C bond formation.

Another transition state **BF_TS3** was found in the reaction of $(CH_3)_3CH + F_2$. The reaction coordinate indicates that this is the transition state for the simultaneous dissociation of the F−F bond and two C−H bonds and formation of two HF molecules. The negative charge on F2 in **BF_TS3** (−0.49e) is not so strong compared with that in **BF_TS2** (−0.88e). The IRC calculation confirms that **BF_TS3** connects **BF_INT** and **BF_PC2**, which is a van der Waals complex of $(CH_3)_2CH{=}CH_2$ and two HF.

The potential energy profile for the reaction of $(CH_3)_3$-$CH + F_2$ is shown in Figure 2. All these intermediates and transition states are more stabilized, relative to the reactants, than in $CH_4 + F_2$: only 0.4 kcal/mol for **BF_RC**, 10.3 kcal/mol for **BF_TS1**, 17.1 kcal/mol for **BF_INT**, 12.9 kcal/mol for **BF_TS2**, and 17.5 kcal/mol for **BF_PC**. The reasons for this larger stabilization may be 2-fold: for one, the C−H bond energy in $(CH_3)_3CH$ (92.5 kcal/mol) is 11.2 kcal/mol weaker that that in CH_4 (103.7 kcal/mol), and second, the interaction in the $(CH_3)_3$-CH species is stronger than that in the CH_4 species due to the electron-donating character of the former. As a result of the largest stabilization, **BF_INT** is more stable than the reactants or reactant complex **BF_RC**, and the reverse barrier from **BF_INT** is now substantial (8.5 kcal/mol). Therefore, this reaction in solution may have to be considered to be a two-step mechanism with the rate-determining barrier of 25.0 kcal/mol for the **BF_INT** → **BF_TS2** step. The barrier is still too high for this reaction to take place under mild conditions. We also note that in Figure 2 the radical dissociation pathway leading to *t*-Bu• + HF + F• from the *t*-Bu···HF···F intermediate **BF_INT** may compete against the ionic pathway for the present system without $CHCl_3$ solvent.

D. Reaction of $(CH_3)_3CH + F_2 + CHCl_3$. Adding one molecule of $CHCl_3$ in the reaction system of $(CH_3)_3CH + F_2$ resulted in two transition states, **BFC_TS1** and **BFC_TS2**, earlier than those without $CHCl_3$, **BF_TS1** and **BF_TS2**, respectively, as shown in Figure 3 and

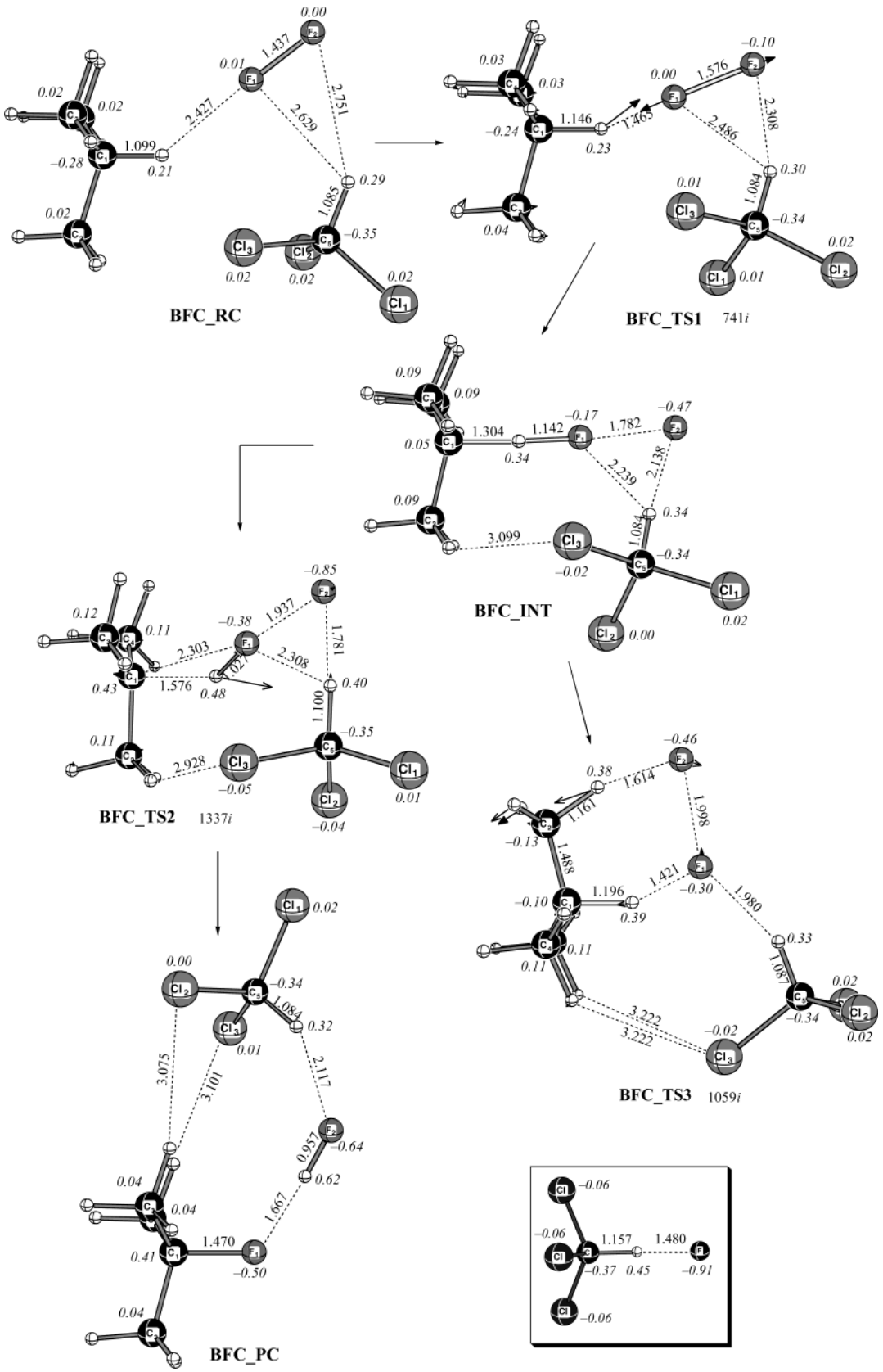

FIGURE 3. Optimized geometries (bond distances in Å) of the stationary points of the reaction of $(CH_3)_3CH + F_2 + CHCl_3$ at the MP2/6-31+(F)G* level. Inset is the optimized geometry of the $Cl_3CH\cdots F^-$ complex. The italic numbers are natural bond orbital atomic charges, except on C where the total charge on the CH_3 group is shown. The imaginary number and arrows on transition state structures give the sole imaginary frequency (in cm^{-1}) and the normal coordinate vector corresponding to this frequency.

sketched in Figure 2. The intermediate **BFC_INT** is also more reactant-like compared with **BF_INT**, with shorter C−H and F−F bonds and a longer H−F bond. In **BFC_TS2**, $CHCl_3$ has very close contact with the strongly negatively charged (−0.85e) F2, with a very small $Cl_3CH\cdots F$ distance of 1.781 Å, while those in all other structures are more than 2.1 Å. The C−H bond of $CHCl_3$ in **BFC_TS2** is also very much stretched to 1.100 Å, in contrast to 1.086 Å in free $CHCl_3$ and similar values in other structures. These distances are just in the middle between the values in the $Cl_3CH\cdots F^-$ complex, 1.480 and 1.157 Å, as shown as an inset in Figure 3, and in other structures. It is interesting to note in Figure 3 that despite this strong $Cl_3CH\cdots F^-$ interaction, the reaction coordinate at **BFC_TS2** remains, as at **BF_TS2**, the rotation of HF so that the proton can be transferred to the negatively charged F2 while F1 forms a bond with the alkyl group.

In **BFC_TS3**, the transition state for the products $(CH_3)_2CH{=}CH_2 + 2HF$, $CHCl_3$ is located at the F1 side with a $Cl_3CH\cdots F^-$ distance of 1.980 Å, and a transfer of negative charge from F2 to F1 is found, i.e., F1 and F2 in **BFC_TS3** have negative charges of −0.30e and −0.46e, respectively, while F1 and F2 in **BF_TS3** have charges −0.24e and −0.49e, respectively. Although we tried to locate $CHCl_3$ at the more negative F2 side, it moved to the F1 side and gave another transition state **BFC_TS3′** in which $CHCl_3$ was located between the C2- and C4-methyl groups (**BFC_TS3′** has an energy 0.2 kcal/mol higher than **BFC_TS3**). In **BFC_TS3**, one of the Cl atoms of $CHCl_3$ interacts with two methyl groups (C3 and C4) with a H···Cl distance of 3.222 Å. Because the other methyl group (C2) rotates to interact with F2, the interaction between the H atom of the methyl group and the Cl atom of $CHCl_3$ is difficult. Thus the approach of $CHCl_3$ to F2 is unfavorable. The reason for the 0.2 kcal/mol higher energy of **BFC_TS3′** compared with **BFC_TS3** is also explainable by the interaction between the methyl group and $CHCl_3$, i.e., only one interaction between the H atom of the C4-methyl group and the Cl atom of $CHCl_3$ is found in **BFC_TS3′**, while **BFC_TS3** has two interactions, C3- and C4-methyl groups.

Addition of $CHCl_3$ in the reaction system of *t*-BuH + F_2 has a drastic effect on the energetics. As shown in Figure 2, $CHCl_3$ stabilizes **BFC_RC**, **BFC_TS1**, **BFC_INT**, **BFC_TS2**, and **BFC_PC** by 3.8, 5.6, 7.9, 17.4, and 5.8 kcal/mol, respectively. These values are substantially larger than the 2.0, 5.0, 5.2, 6.9, and 4.9 kcal/mol values for **MFC_RC**, **MFC_TS1**, **MFC_INT**, **MFC_TS2**, and **MFC_PC**, respectively, in the CH_4 + F_2 reaction. As expected from the structural evidence of the strong $Cl_3CH\cdots F^-$ interaction shown above, the stabilization of the key transition state **BFC_TS2** is dramatic. This reduces the rate-determining barrier at the **BFC_INT** → **BFC_TS2** step to 15.6 kcal/mol, into the range that makes the reaction feasible under mild conditions.

The activation barrier for **BF_INT** → **BF_TS3**, 26.6 kcal/mol, is comparable to that of **BF_INT** → **BF_TS2**, 25.0 kcal/mol. The stabilization effect of adding $CHCl_3$ to **BF_TS3** is small, because the charge separation on F2 is small in **BF_TS3**, −0.49e, compared with **BF_TS2**, −0.88e. Thus the activation barrier of **BFC_INT** → **BFC_TS3**, 26.1 kcal/mol, is almost unaffected by adding $CHCl_3$, while that for **BFC_INT** → **BFC_TS2**, 15.6 kcal/mol, becomes smaller. Hence the elimination reaction to produce $(CH_3)_2C{=}CH_2$ is not competitive with the fluorination reaction in the presence of $CHCl_3$. We also note that in Figure 2 the radical dissociation pathway leading to *t*-Bu$^\bullet$ + HF + F$^\bullet$ from the *t*-Bu···HF···F intermediate **BFC_INT** becomes less competitive against the ionic pathway for the present system in the presence of one molecule of $CHCl_3$ solvent.

E. Reaction of CH_4 or $(CH_3)_3CH + F_2 + nCHCl_3$ (n = 1−3). As is seen above, addition of one $CHCl_3$ molecule in the calculation for the $(CH_3)_3CH + F_2$ reaction system dramatically changes the potential energy profile of the reaction. An inspection of the structure of the key transition state **BFC_TS2** in Figure 3 suggests that the anionic F2, strongly interacting with one molecule of $CHCl_3$, still has a large free area on the opposite side of the approaching $CHCl_3$, and more $CHCl_3$ molecules may interact with it to further stabilize this transition state. To evaluate the effects of the additional $CHCl_3$ molecules, ONIOM(MP2/6-31+G*:HF/6-31+G*) calculations were carried out for CH_4 and $(CH_3)_3CH + F_2 + n CHCl_3$ (n = 1−3), using CH_4 and $(CH_3)_3CH + F_2 + n HF$ as the ONIOM "model" system, respectively. In these systems, we did not carry out calculations for the product complexes **PC**, since they are very low in energy and have no direct relevance to the rate of reaction.

The optimized geometries of stationary structures for n = 3 are shown in Figure 4, while those for n = 1 and 2 are given in Figures S5 and S6 in the Supporting Information. The structures in Figure 4 show that the reacting H···F···F region of the system is surrounded by these three $CHCl_3$ molecules and the first solvation shell is nearly completed. For the reaction of $(CH_3)_3CH + F_2 + CHCl_3$, one can compare the ONIOM(MP2/6-31+G*:HF/6-31+G*) optimized geometries with those from MP2/6-31+(F)G*. The geometries of *t*-Bu−H−F−F part of the stationary points of this reaction by the two methods are close to each other, except for the F−F bond length in **BFC1_INT**, where the ONIOM value is 0.036 Å longer than that from MP2. All stationary points obtained by ONIOM(MP2/6-31+G*:HF/6-31+G*) are more reactant-like with the increasing number of $CHCl_3$ molecules except for the **INT**; the F−F bond length in **INT** increases with the number of $CHCl_3$ molecules. The $Cl_3CH\cdots F$ distance increases with the number of $CHCl_3$ molecules at all stationary points. Table 1 shows the activation energies calculated by ONIOM for various solvated systems, compared with the MP2 results for smaller systems. We could not locate the intermediates in the case of MeH. Because the activation energy of the second step, E(**INT**→**TS2**), should be larger than the energy difference between **TS2** and **TS1**, these energy differences were shown as the lowest limits of E(**INT**→**TS2**). In the case of *t*-BuH, the E(**INT**→**TS2**), was dramatically decreased with the increasing number of $CHCl_3$. The E(**INT**→**TS2**) of the reaction of *t*-BuH + F_2 + 3$CHCl_3$ is 5.2 kcal/mol, and it is low enough for this reaction to take place under mild conditions.

Figure 5 shows the potential energy profiles for the reaction of MeH and *t*-BuH. Addition of $CHCl_3$ in the reaction system stabilizes all stationary points and the stabilization effect increases in the order of **RC** < **TS1** < **INT** < **TS2**. Especially, the **TS2** of the reaction of

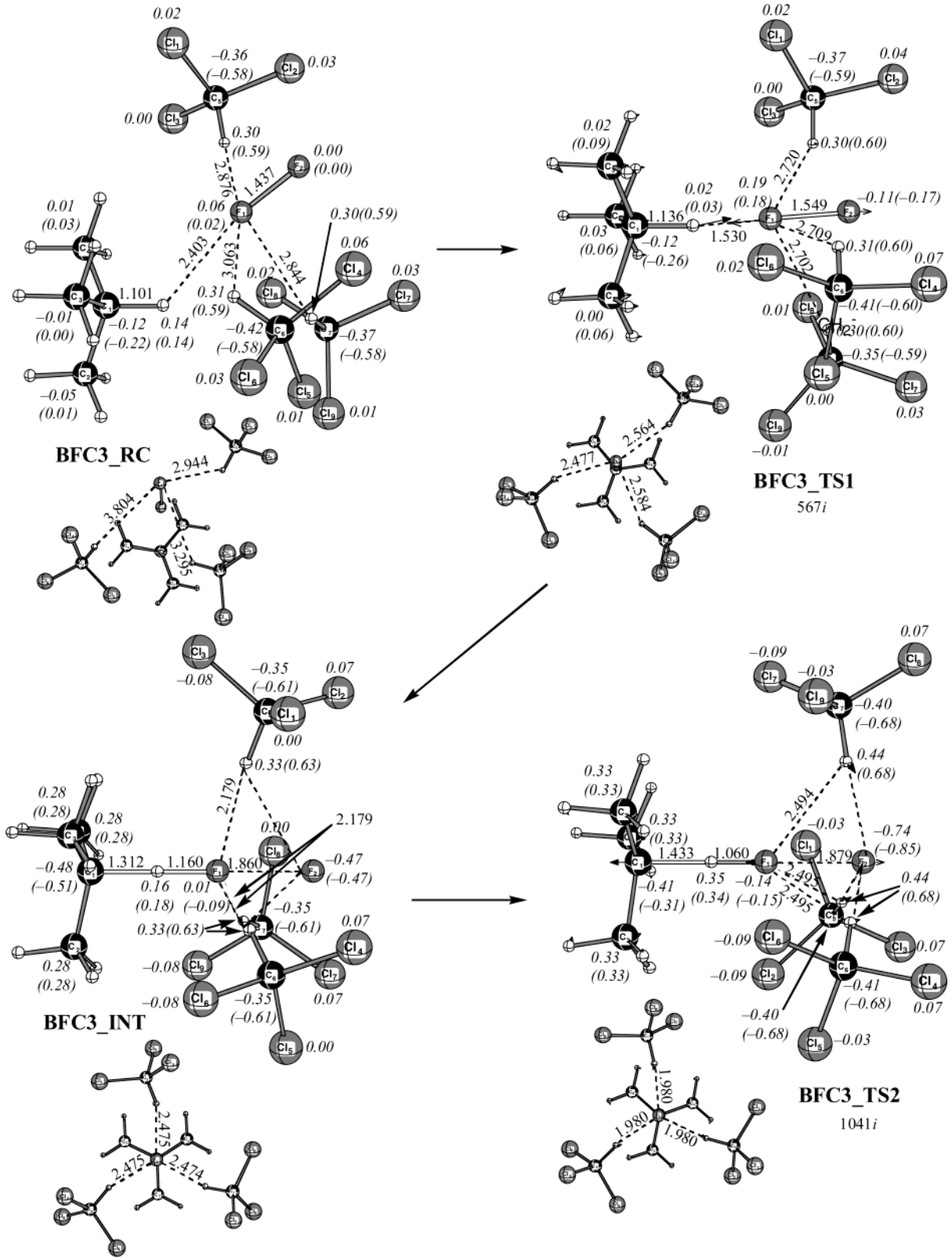

FIGURE 4. Optimized geometries (bond distances in Å) of the stationary points of the reaction of $(CH_3)_3CH + F_2 + 3CHCl_3$ at the ONIOM(MP2/6-31+G*:HF/6-31+G*) level. For details, see the caption of Figure 3. The italic numbers are Mulliken atomic charges, except on C where the total charge on the CH_3 group is shown. Mulliken charges in "model" systems are shown in parentheses.

t-BuH + F_2 is still largely stabilized by second and third $CHCl_3$ molecules, i.e., 11.1 and 7.9 kcal/mol, respectively. Figure 5 shows clearly, once three $CHCl_3$ solvent molecules participate in the reaction, the entire reaction: *t*-BuH + F_2 → *t*-BuF + HF becomes a very easy process, the barriers for the two steps of the reaction are reduced

TABLE 1. MP2 and ONIOM Activation Energies (in kcal/mol) for CH_4 and $(CH_3)_3CH + F_2 + nCHCl_3$ Reaction Systems

reaction	method	*E*(**RC**→**TS1**)	*E*(**INT**→**TS2**)	*E*(**RC**→**TS2**)
$MeH + F_2$	MP2/6-31+G*//MP2/6-31+(F)G*	15.6	20.8	34.7
$MeH + F_2 + CHCl_3$	MP2/6-31+G*//MP2/6-31+(F)G*	12.6	19.1	29.8
$MeH + F_2 + CHCl_3$	ONIOM(MP2/6-31+G*:HF/6-31+G*)	13.5	>17.0	30.4
$MeH + F_2 + 2CHCl_3$	ONIOM(MP2/6-31+G*:HF/6-31+G*)	11.5	>16.0	27.5
$MeH + F_2 + 3CHCl_3$	ONIOM(MP2/6-31+G*:HF/6-31+G*)	11.0	>12.9	23.9
t-$BuH + F_2$	MP2/6-31+G*//MP2/6-31+(F)G*	5.7	25.1	22.2
t-$BuH + F_2 + CHCl_3$	MP2/6-31+G*//MP2/6-31+(F)G*	3.9	15.6	8.6
t-$BuH + F_2 + CHCl_3$	ONIOM(MP2/6-31+G*:HF/6-31+G*)	4.2	16.3	9.7
t-$BuH + F_2 + 2CHCl_3$	ONIOM(MP2/6-31+G*:HF/6-31+G*)	3.3	9.3	−0.5
t-$BuH + F_2 + 3CHCl_3$	ONIOM(MP2/6-31+G*:HF/6-31+G*)	2.5	5.2	−7.7

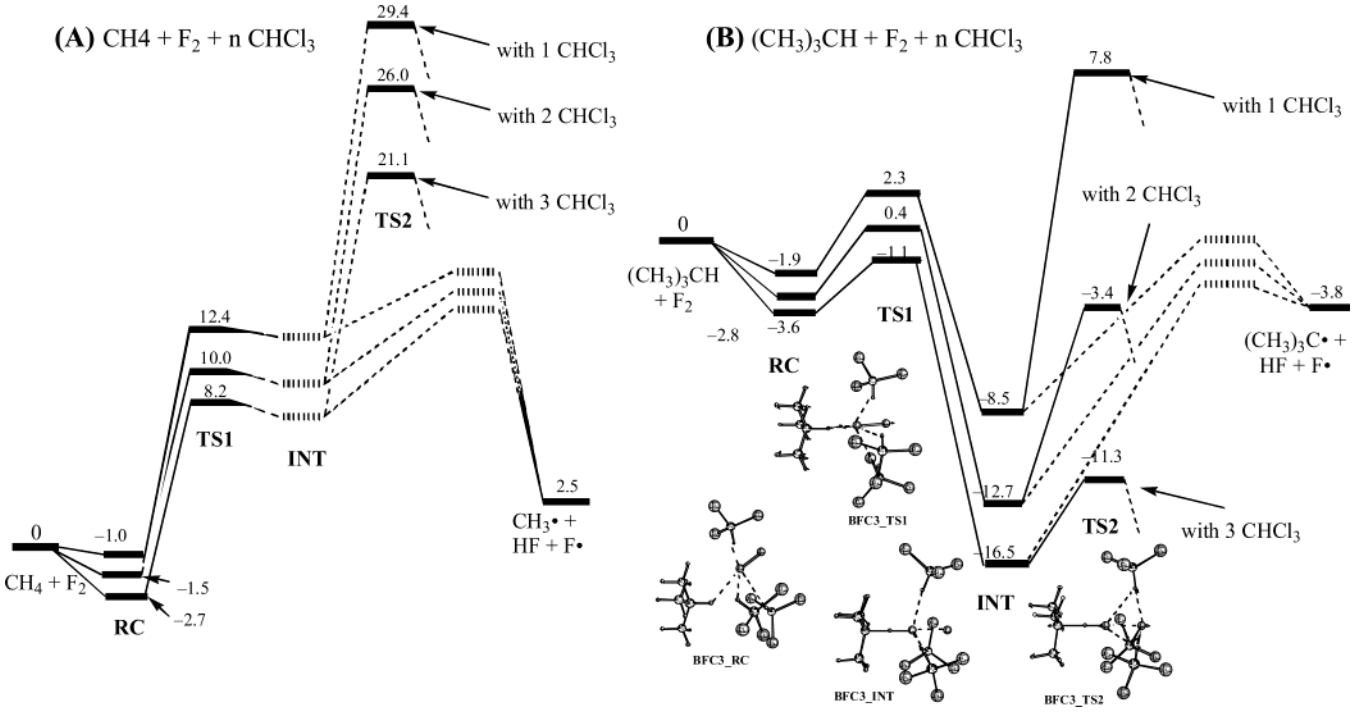

FIGURE 5. Potential energy profiles (in kcal/mol, with ZPE) for the reaction of (A) $CH_4 + F_2 + nCHCl_3$ and (B) $(CH_3)_3CH + F_2 + nCHCl_3$, for $n = 1$, 2, and 3, at the ONIOM(MP2/6-31+G*:HF/6-31+G*) level. Note the two figures have difference energy scales. Sketches of the structures are for $(CH_3)_3CH + F_2 + 3CHCl_3$ taken from Figure 4.

to 4.7 and 5.2 kcal/mol, and the reaction becomes a very easy reaction. Thus in the case of *t*-$BuH + F_2 + 3CHCl_3$, the ionic process was preferred to the radical one, because the **TS2**, −11.3 kcal/mol, was sufficiently lowered to prevent production of the radical pair of *t*-$Bu^{\bullet}$ + HF + $F^{\bullet}$, −3.8 kcal/mol, from the intermediate **INT**.

The origin of the energy lowering of **INT** and, in particular, the second transition state **TS2** is quite obvious from the findings and discussions above. NBO analysis indicates that these species are very highly ionic in nature, although substantial delocalization of the charges is still seen and far from the pure ion-pair, and the solvation by the polar $CHCl_3$ molecules at the most polar region of the species stabilized these species. The structures in Figure 4 suggest that with three $CHCl_3$ molecules, the first solvation shell is nearly completed, and the effects of additional $CHCl_3$ molecules on the potential energy surface are expected to be substantially smaller.

Concluding Remarks

We have examined the monofluorination reaction of methane and isobutane by F_2 with and without $CHCl_3$ solvent molecules by using the MP2 and ONIOM methods. The followings are conclusions.

(1) The electrophilic pathway for the $RH + F_2$ reaction in general is a two-step process, consisting of hydride abstraction leading to an intermediate of the type $R^{+\delta}\cdots HF\cdots F^{-\delta}$, followed by its complicated rearrangement to give the electrophilic substitution product, RF + HF. The configuration of the alkyl group is fully retained during this two-step electrophilic reaction.

(2) In the reaction of $MeH + F_2$, the overall activation process should be considered to be a single step from the reactant complex **MF_RC** to the second transition state **MF_TS2**, because the reverse barrier from the intermediate **MF_INT** to the first transition state **MF_TS1** is so small (1.7 kcal/mol). The overall barrier from **MF_RC** to **MF_TS2**, 34.7 kcal/mol, is too high to take

place under mild conditions. Although addition of $CHCl_3$ in the reaction system lowers the overall barrier of **MFC_RC** → **MFC_TS2** to 29.8 kcal/mol, it is still too high to occur.

(3) In the reaction of *t*-BuH + F_2, the intermediate **BF_INT** is substantially stabilized to prevent the reverse reaction from **BF_INT** to **BF_TS1**. So, this reaction is actually considered to be a two-step mechanism: the activation barrier for the first step is 5.7 kcal/mol and that for the second one is 25.0 kcal/mol. However, the rate-determining barrier of 25.0 kcal/mol is still too high to occur under mild conditions.

(4) The charge separations of the stationary points increases in the order of **RC** < **TS1** < **INT** < **TS2**, especially in the case of isobutane, because the electron-donating character of the three methyl groups of *t*-Bu assists the electron transfer to the fluorine atoms. The most polar species **TS2** is highly stabilized by $CHCl_3$, and therefore the rate-determining barrier of the reaction of *t*-BuH + F_2 + $CHCl_3$ become 15.6 kcal/mol.

(5) In the case of isobutane, solvation of the reaction system by three molecules of $CHCl_3$, *t*-BuH + F_2 + $3CHCl_3$, the ionic process becomes strongly preferred to the radical one and the barrier for the ionic process becomes very low so that the electrophilic substitution takes place in mild conditions. Specifically **TS2** is sufficiently lowered, −11.3 kcal/mol, to prevent the production of the radical pair of *t*-Bu$^{\bullet}$ + HF + F$^{\bullet}$, −3.8 kcal/mol, from **BF_INT**. This electrophilic substitution of *t*-C−H to *t*-C−F by F_2 in $CHCl_3$ solvent occurs with full retention of configuration.

In the present paper, we are very much interested the participation of the solvent molecule in the reaction, and the microsolvation model used here is ideally suited for this purpose. An alternative approach is continuum models in which the bulk solvent is approximated by a polarizable continuum. The latter approach may be more suitable for simulation of the reaction in solution, but loses all the specific interactions. A best approach would be a combination of microsolvation and continuum, with a few solvent molecules explicitly included in the model that is surrounded by the continuum. In the case where the micro-solvation model was treated by the ONIOM method, as in our case of $(CH_3)_3CH$ + HF + $n CH_3Cl$, the ONIOM-PCM method that allows the ONIOM molecule surrounded by a continuum is needed.[15] Such a method is just becoming practical and will be used in a future study.

Acknowledgment. The authors are grateful to Dr. S. Rozen for suggesting this study and helpful discussions. H.F. acknowledges the STA (Science and Technology Agency of Japan) fellowship for visiting Emory University. Acknowledgment is made to the Cherry L. Emerson Center of Emory University for the use of its resources, which is in part supported by a National Science Foundation grant (CHE-0079627) and an IBM Shared University Research Award. Acknowledgment is also made to the Tsukuba Advanced Computer Center of AIST.

Supporting Information Available: Figure S1 showing the optimized geometries and their relative energies of **TS2** for the reaction of $(CH_3)_3CH$ + F_2, obtained at various theoretical levels; Table S1 giving the relative energies of two transition states in MP2/6-31+G* and MP2/6-31+(F)G* optimization and single-point energy; Table S2 giving the relative energies for the $(CH_3)_3CH$ + F_2 + $CHCl_3$ system, as a test of ONIOM models and methods; Figure S2 showing the optimized geometries of the stationary points of the reaction of CH_4 + F_2 at the MP2/6-31+(F)G* level; Figure S3 showing the optimized geometries of the stationary points of the reaction of CH_4 + F_2 + $CHCl_3$ at the MP2/6-31+(F)G* level; Figure S4 showing the optimized geometries of the stationary points of the reaction of $(CH_3)_3CH$ + F_2 at the MP2/6-31+(F)G* level; Figures S5 and S6 showing the optimized geometries of the stationary points of the reaction of $(CH_3)_3CH$ + F_2 + $nCHCl_3$ at the ONIOM(MP2/6-31+G*:HF/6-31+G*) level, for $n = 1$ and 2, respectively; Table S3 giving the Z matrix of all the structures optimized at the MP2/6-31+G*//MP2/6-31+(F)G* level; and . Table S4 giving the Cartesian coordinates of all the structures optimized at the ONIOM(MP2/6-31+G*:HF/6-31+G*) level. This material is available free of charge via the Internet at http://pubs.acs.org.

JO034740C

(15) (a) Vreven, T.; Mennucci, B.; da Silva, C. O.; Morokuma, K.; Tomasi, J. *J. Chem. Phys.* **2001**, *115*, 62. (b) Mo, S. J.; Vreven, T.; Mennucci, B.; Morokuma K.; Tomasi, J. *Theor. Chim. Acc.* In press.